Cell culture analysis through learning-enabled lens-free microscopy

Florian Lemarchand[1]   Chiara Paviolo[1]   Lionel Hervé[1]   Lamya Ghenim[2]
Kiran Padmanabhan[3]   Cédric Allier[1,*]

[1]Univ. Grenoble Alpes, CEA, Leti, F-38000 Grenoble

[2]Univ. Grenoble Alpes, INSERM, CEA-IRIG, BGE, Biomics, Grenoble, F-38000

[3]Institut de Génomique Fonctionnelle de Lyon, CNRS UMR 5242, Ecole Normale Supérieure de Lyon, Université Claude Bernard Lyon 1, Lyon, France

* C. Allier was affiliated with CEA-Leti at the time of the study; he is currently affiliated with Howard Hughes Medical Institute, Janelia Research Campus.

Résumé – Un imageur sans lentille est un dispositif de microscopie effectuant des mesures holographiques. Ce dernier de par son large champ de vue permet d'imager des cultures cellulaire sur une surface de 30 mm² sur plusieurs jours. Ces dernières années, l'analyse d'image a rapidement évolué en profitant des avancées des algorithmes par apprentissage. Couplés à un imageur sans lentille ces algorithmes permettent d'effectuer des mesures quantitatives sur des cellules uniques au sein de larges populations (>10.000). Nous proposons ici une solution intégrant l'analyse morphologique et temporelle, afin d'extraire la description d'une culture de cellules HeLa. Notre approche permet de mesurer automatiquement des paramètres liés aux cycles de division cellulaire.

Abstract – A lens-free microscope is a device performing holographic measurements. Its large field of view allows one to image cell cultures on a surface of 30 mm² over several days. In recent years, image analysis has evolved rapidly by taking advantage of advances in learning algorithms. Coupled to lens-free imaging, these algorithms enable wide field quantitative measurements on single cells within large populations (>10.000). We propose here a solution integrating morphological and temporal analysis to gather the description of a HeLa cell culture. Our approach allows to measure metrics related to cell division cycles.

1   Introduction

Recent advances in bioimaging have allowed the visualization and the quantification of novel spatial and temporal cellular features, thus increasing exponentially the amount of available data for analysis [1]. These requirements translate into the need for more complex imaging analysis pipelines to quantify the dynamics present in the biological models. Deep Learning (DL) methods have been shown to be capable of extracting cellular features and often outperform standard image-processing strategies in terms of performance and computational speed [2]. The most diffused algorithms for image analysis are currently Convolutionnal Neural Network (CNN), which learns how to extract targeted parameters directly from raw data by using multiple linear and/or non-linear transformations [3]. Typical tasks now performed by CNNs include image segmentation, cellular tracking, quantification of features, and image classification [1]. Recently, generalist pre-trained models have been used as analysis tools to facilitate image analysis and cell detection [4, 5]. While these models are generalist, i.e. trained on large databases of highly variable data, they need to be adapted to a specific dataset with a human-in-the-loop pipeline [6].

We present here a novel pipeline that performs single-cell analysis and feature quantification on time-lapses of lens-free microscopy images. The challenge lies in adapting neural networks solution to this modality, the acquisitions being not well resolved and the field of view being ten folds larger in comparison with the microscopy techniques. Feature extraction is based on algorithms for cell segmentation [5] and tracking. To improve the segmentation algorithm, a human-in-the loop

approach [6] has been used to adapt to the data to be analysed. Different types of features are extracted, including morphology, kinetics or cell-to-cell division metrics. The large field of view of the lens-free microscope enables the analysis of thousands of cells per frame. In addition, the use of time-lapses scales the number of cell instances under analysis in the million range and cell tracking enables life-long metric extraction for cell-division cycles. This proof-of-concept has been conducted on a standard cell culture model to build up a gold reference for more heterogeneous cell culture conditions.

2   Materials and Methods

This section presents the methods proposed to analyse a cell culture time-lapse, as well as the cell line used for experiments.

2.1   HeLa Cell Culture

HeLa cells were cultured in high glucose DMEM supplemented with GlutaMAX, pyruvate, 10% calf serum (Gibco) and 1% penicillin/streptomycin (Invitrogen). Hela is an immortalized cell line derived from cervical cancer cells.

2.2   Lens-free Imaging

Images were acquired in a cell culture incubator every 10 minutes for three days on a lens-free microscope (Iprasense, FR) as previously described [7]. In brief, the microscope features an Red Green Blue (RGB) LED source that directly illuminates the sample located on a CMOS detector (3840 x 2748 pixels of $1.67\mu m$ pitch, for a total imaging area of 29.4 mm²). The lens-free setup records intensity-only measurements at the sensor plane. Three different diffraction patterns

RGB are then processed to reconstruct Optical Path Difference (OPD) and absorption images [8]. This process is based on an inverse problem optimization improved by a CNN iteration. Data fidelity is guaranteed by a second inverse problem optimization using the prediction from the CNN as initialization of the algorithms. The process can be further accelerated to 3 s per image by performing CNN-based phase unwrapping [7]. In Figure 2a the top left quarter of the image is the output of the lens-free image reconstruction. Measurements of dry mass are acquired with a precision of approximately 35 pg [9].

2.3 Analysis Pipeline

The analysis pipeline consists of two parts. First a segmentation pipeline is applied frame by frame to detect individual cells. Second, a tracking algorithm links detections related to cell instances. Segmentation masks and temporal tracks are analysed to obtain morphological and temporal metrics of the entire cell population at single-cell level.

Detection/Segmentation Cellpose [5] has been used for cell detection and segmentation. Cellpose is a deep neural network for segmentation. Its architecture has a U-Net style and contains residual blocks. We used the publicly released code for running Cellpose. Here, we leveraged the human-in-the-loop faculty of the package to train a segmentation model dedicated to our data. The fine-tuning process started from the predictions of the "Cyto" pre-trained model of Cellpose. 256×256 pixels patches were extracted from the images of the dataset to be segmented. 5 images were picked at different cell concentrations in the range of 100-500 cells/mm² (empirically selected limits to avoid high cell concentrations and superposition of the cell borders). The patches were then used as training samples in the Cellpose human-in-the-loop interface. Precision and recall were measured at each training step. The training process stopped when no detection improvements were observed. The ground-truth positions were manually generated using the CellCounter plugin of FIJI [10]. At the end of the training, 0.99 precision and recall scores are reached on an evaluation set which contains 1320 cells at a density of 500 cells/mm². The ground-truth masks for segmentation evaluation were outlined manually using the Cellpose interface. The average Intersection over Union (IoU) on an evaluation set of 221 cells at a density of 500 cells/mm² is 0.8.

Once the model is trained, segmentation masks for all the frames of the time-lapse are predicted. Figure 2a top-right quarter displays the masks predicted by the segmentation model. From these predictions different features are measured directly from the masks including: centroid coordinates, dry mass, area, thickness, axis lengths. The major and minor axis lengths are measured by fitting an ellipse to the cell masks. At this point, frame-wise features can also be measured to obtain global and neighbouring cell densities.

Figure 1 displays box-plots representing the errors of the analysis pipeline. Cell features are overall under-estimated, i.e. predicted values tends to be smaller than ground-truths. Indeed, the main drawback of the analysis is the correct segmentation of cell protrusions. Interestingly, Figure 1 shows zero 5th to 95th percentil errors for thickness analysis. Thickness is calculated from the maximum value of the cell-masked OPD which often lies in the center of the mask, leading to measured values that perfectly match the ground-truth.

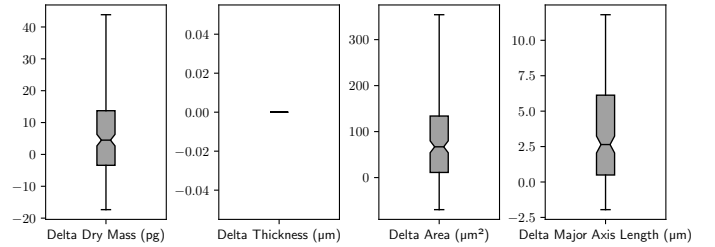**Tracking** Once the masks of the whole time-lapse are pre-

Figure 1 – Evaluation of measurements errors. Values are the difference between features measured from manual annotation and measured from the fine-tuned Cellpose model. The box-plots display from bottom to top: the 5th, 25th, 75th and 95th percentils of errors. The notch represents the median value.

dicted, the tracking algorithm links individual instances corresponding to the same cell. For this purpose, the TrackPy library was used [11]. TrackPy is a Python implementation of the Crocker–Grier algorithm [12]. The tracking was computed with respect to spatial coordinates from one frame to the next. A threshold of $D = 23 \mu m$ has been applied to the pairing distance in order to limit cell displacements between consecutive frames. The threshold has been selected empirically to be as large as the maximum displacement observed in the whole time-lapse. A gap-closing parameter of 3 frames ($C = 3$) was used to link individual cell instances. This parameter avoids the tracking to terminate when an occlusion occurs, i.e. when a cell detection is missing on individual frames. The pairing is constrained by a threshold $\Delta_{DM} = 150 pg$ on the cell dry mass evolution which enables track splitting when cell division occurs. The cell dry mass is expected, indeed, to halve as a cell divides.

The track splitting at division events makes it possible to gather cell-division cycle features like, initial and final dry mass, the time between consecutive divisions, and cell displacements. For this purpose, only complete cell-division cycles (i.e. from one cell division to the next) were analysed, therefore excluding: i) incomplete tracks starting or lasting outside the imaging time, and ii) tracks containing detections closer than $25 \mu m$ from the frame border (to avoid cells entering and exiting the field of view). A threshold of 5 hours has been applied to the data, according to published distributions on cell-division duration related to different cell lines [9].

3 Experiments

This section presents the analysis of a HeLa cell culture using the proposed method. The analysis is made on a time-lapse of 436 images of resolution 3840 x 2748 acquired with a time step of 10 minutes. This time-lapse represents an acquisition of more than three days. At the beginning of the acquisition, the field of view includes 1700+ cells, whose consecutive divisions led to 22000+ cells in the end. Overall, we were able to detect around 4 million instances in this time-lapse.

3.1 Population Analysis

To retrieve the morphological information, first we gathered together all the features extracted from the cell segmentation masks. Figure 2a shows a full frame image with colour-coded masks of measured areas and dry masses (bottom-left and right quarters, respectively). The analysis of individual morpholog-
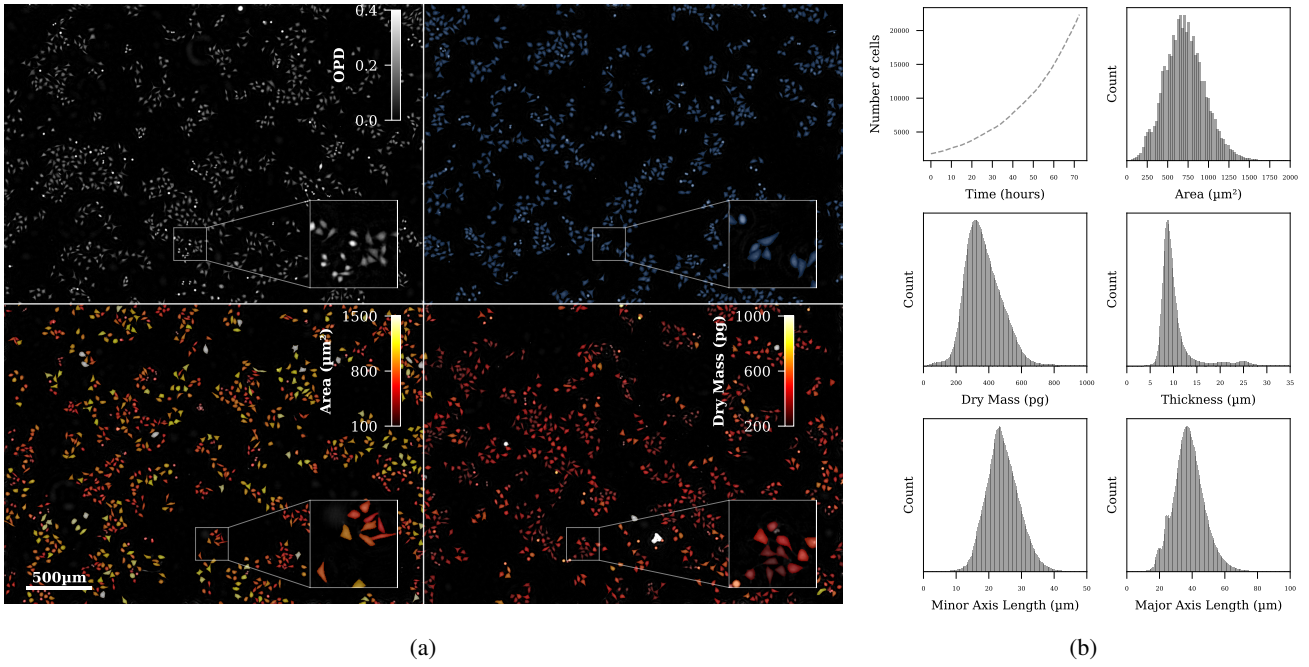
(a)

(b)

Figure 2 – (a) A full field frame extracted from time $t = 21h$ 40m. The frame contains 4000+ cells corresponding to a cell density of 135 cells/mm². Top-left: reconstructed phase image, i.e. the OPD; top-right: binary output of segmentation; bottom-left: segmentation masks coding the measured area of the underlying cell; bottom-right: segmentation masks coding the measured dry mass of the underlying cell. (b) Single-cell analysis of a complete time-lapse lasting 70+ hours. 4M+ detection instances are measured.
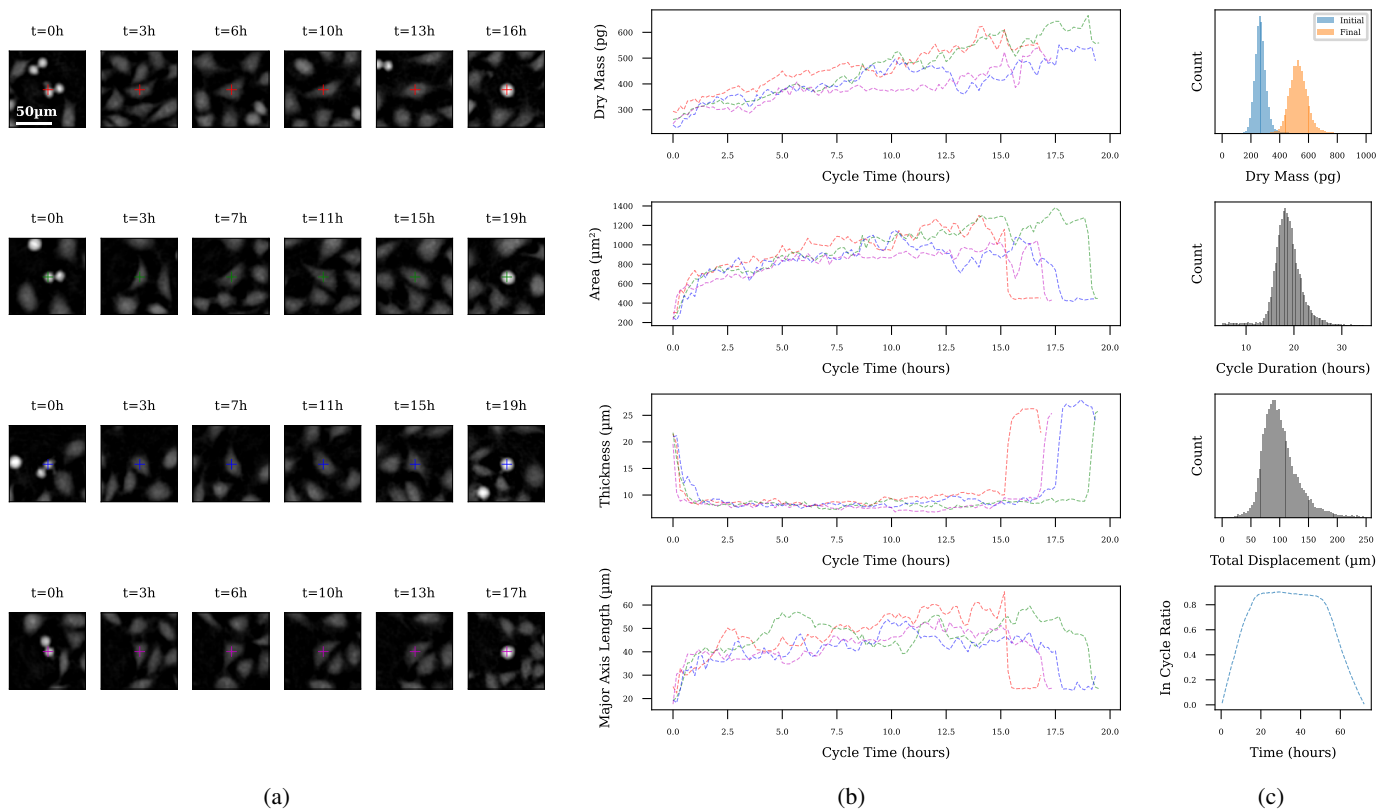

(a)

(b)

(c)

Figure 3 – (a) Display of the cell cycle progression at 6 different times for four different cells. The cursors show the position of each cell of interest (identified by the color of the cursor). (b) Dry mass, area, thickness and major axis length, measured by our method, versus time. The colors in each curve correspond to the cells as identified in (a). (c) Cycle-wise analysis. From top to bottom: the first plot displays the histograms of cell dry mass measured at the beginning and at the end of the cycles. The second is the histogram of cycle duration. The third plot displays the histogram of displacement sum through cell life, i.e. total displacement during a cell cycle. The last plot shows the ratio of cells under analysis (i.e. in a complete cycle) with respect to the number of detected cells.

3

ical features is depicted in Figure 2b. Overall, the data are normally distributed over the entire time-lapse, therefore showing a good homogeneity of the cell population. As expected, the cell number increased exponentially over the analysed time-lapse. It is interesting to see that the analysis is precise enough to highlight the difference in shape between mitotic cells (spherical shape) and adherent cells. This can be deduced from the 3 peaks appearing in the thickness analysis. First the major peak corresponds to the thickness of adherent cells. Then the two peaks at $21\mu m$ and $25\mu m$ coincide with the thicknesses of cells, right before and after mitotic event, respectively. These values can also be observed in Figure 3b, the second row with $21\mu m$ and $25\mu m$ thicknesses at the beginning and end of cycles, respectively. Interestingly, the same observation applies to major axis length measurements with peaks at 20 and $23\mu m$. These two values are close to the mean of the minor axis lengths, representing indeed the rounded-shape cell population.

3.2 Temporal Analysis

Our tool makes it possible to go further than a simple population analysis. In fact, we are able to track the cells in time and then conduct temporal analysis, population-wise or division cycle-wise.

Figure 3a shows image cropped from four different cell-division cycles while Figure 3b displays the corresponding features monitored over time. The display of each cell at six different positions shows that the cycles are well detected from mitosis to mitosis (i.e. where a cell goes under spherical configuration). As the cell grows, the monitoring of the cell features confirms the increasing of dry mass over time, and the correct definition of the mitotic events (corresponding to a decrease in the cell surface area, increase of the cell thickness and decrease of the major axis length).

Figure 3c shows the quantification of different cell-division based features (namely the initial and final dry mass, the cell cycle length and the total cell displacement). These graphs describe the overall cell population, giving important information on the homogeneity of the cell culture. The initial dry mass roughly doubled over the cell-division cycle. This behaviour is in good agreement with previously published analysis from images acquired with a high resolution setup [13]. We observed a mean cell-division duration of 18.5 hours, in fair agreement with other published data on HeLa cells [9]. Importantly, we can also estimate the ratio of the number of cells detected at each point of the time-lapse and the number of cells under complete-cycle analysis (bottom graph in Figure 3c). Overall, the ratio of cells under analysis is over 0.88, which indicates that the greater majority of the cells have been analysed.

4 Conclusion

This paper presents a method designed for the quantitative analysis of cell culture time-lapses acquired using a lens-free microscope. The method has been applied to a HeLa cell culture as a test experiment. Importantly, we show the extraction of morphological and temporal features on more than 4 million cells, gathering information on the homogeneity of the culture. Overall, the data shows that the different extracted features are maintained over many generations, despite the biological variability that can occur over different cell cycles.

This work opens up novel directions for the analysis of cell behaviour for different cell types and morphology. The features extracted by the proposed pipeline may be used as training sets for algorithms predicting directly cell quantitative features from phase images. The large number of measurement points opens up the prospect of graph neural network modeling of cell cultures.

5 Acknowledgments

References

[1] E. Moen, D. Bannon, et al. Deep learning for cellular image analysis. *Nature Methods*, 16(12):1233–1246, December 2019.

[2] L. Von Chamier, R.F. Laine, et al. Democratising deep learning for microscopy with ZeroCostDL4Mic. *Nature Communications*, 12(1):2276, April 2021.

[3] J.C. Caicedo, S. Cooper, et al. Data-analysis strategies for image-based cell profiling. *Nature Methods*, 14(9):849–863, September 2017.

[4] U. Schmidt, M. Weigert, et al. Cell Detection with Star-Convex Polygons. In *Medical Image Computing and Computer Assisted Intervention – MICCAI 2018*, Lecture Notes in Computer Science, pages 265–273, Cham, 2018. Springer International Publishing.

[5] C. Stringer, T. Wang, et al. Cellpose: a generalist algorithm for cellular segmentation. *Nature Methods*, 18(1):100–106, January 2021.

[6] M. Pachitariu and C. Stringer. Cellpose 2.0: how to train your own model. *Nature Methods*, 19(12):1634–1641, December 2022.

[7] C. Allier, L. Hervé, et al. CNN-Based Cell Analysis: From Image to Quantitative Representation. *Frontiers in Physics*, 9, 2022.

[8] L. Hervé, D. C. A. Kraemer, et al. Alternation of inverse problem approach and deep learning for lens-free microscopy image reconstruction. *Scientific Reports*, 10(1):20207, November 2020.

[9] L. Ghenim, C. Allier, et al. A new ultradian rhythm in mammalian cell dry mass observed by holography. *Scientific Reports*, 11(1):1290, January 2021.

[10] J. Schindelin, I. Arganda-Carreras, et al. Fiji: an open-source platform for biological-image analysis. *Nature Methods*, 9(7):676–682, July 2012.

[11] D.B. Allan, T. Caswell, et al. soft-matter/trackpy: v0.6.1, February 2023.

[12] J. C. Crocker and D. G. Grier. Methods of Digital Video Microscopy for Colloidal Studies. *Journal of Colloid and Interface Science*, 179(1):298–310, April 1996.

[13] X. Liu, S. Oh, L. Peshkin, et al. Computationally enhanced quantitative phase microscopy reveals autonomous oscillations in mammalian cell growth. *Proceedings of the National Academy of Sciences*, 117(44):27388–27399, November 2020.